JOURNAL OF MATERIALS SCIENCE 32 (1997) 4723–4729

Microstructure of TiNi shape-memory alloy synthesized by explosive shock-wave compression of Ti–Ni powder mixture

XIAODONG HAN*‡
Department of Materials Science, Dalian University of Technology, Dalian 116024, People's Republic of China

WENHUI ZOU*, RENHUI WANG*
Department of Physics, Wuhan University, Wuhan 430072, People's Republic of China

SING JIN, ZE ZHANG
Beijing Laboratory of Electron Microscopy, Chinese Academy of Science, Beijing 100080, P.O. Box 2724, People's Republic of China

TONGCHUN LI, DAZHI YANG
Department of Materials Science, Dalian University of Technology, Dalian 116024, People's Republic of China

Cylinders of TiNi shape-memory alloy were synthesized from mixtures of equiatomic fine irregular titanium and nickel powders by explosive-wave compression with a detonation velocity of about 6500 m s^{-1}. B2 type parent phase, R phase, B19′ type martensite, Ti_2Ni, Ti_3Ni_4 and Ti_2Ni_3 phases were observed in this as-synthesized material. In the B2 matrix high density dislocations existed. The Burgers vectors of many dislocations were determined to be parallel to $\langle 1\,1\,1 \rangle$ directions. The R phase variants formed (0 0 1) B2 twinning structure. The substructure of the B19′ martensite was (0 0 1) B19′ type I twin and stacking faults on the (0 0 1) B19′ plane. When increasing the temperature of the as-synthesized material in a differential scanning calorimeter, no B19′ → R → B2 transitions were observed on the temperature range −50 to 100 °C. However, B2 → B19′(R) transitions occurred during the cooling cycle. After heat treating the specimen at 800 °C for 1 h and then ageing at 400 °C for 10 min, both B2 → R → B19′ and B19′(R) → B2 phase transitions were observed.

1. Introduction

TiNi shape-memory alloy (SMA) is an excellent functional material. It has many good characteristics, such as perfect shape-memory effect (SME), superelasticity and high corrosion resistance. However, its high price, resulting from complicated and difficult melting and machining procedures, have limited its application. In order to utilize TiNi SMA cheaply and widely, many manufacturing methods, such as powder metallurgy [1], self-propagating high-temperature synthesis (SHS) [2], which can omit many complicated processes, have been tried. In recent years, explosive shock-initiated chemical reactions are of considerable interest. With the high temperature and pressure associated with shock-wave processing, it may concurrently synthesize and form net-shaped parts of intermetallic compounds and other materials from elemental powders. Shock compression of powders produces an unusual combination of "structure defects" and "powder packing characteristics" that can significantly promote chemical reactivity of powders and lead to accelerated mass transport kinetics. Under such unique conditions, not only can metal and ceramic powders be dynamically consolidated [3, 4], or undergo solid-state phase transformation [5], but also molecular decomposition of compounds can occur [6], as well as chemical reactions in bonding mixtures [7], resulting in the synthesis of compounds. We have tried a technique of obtaining TiNi SMA directly by means of explosive shock-wave compression which induce chemical reaction in an equiatomic Ni/Ti powder mixture. The detailed microstructure and phase transformation behaviour of the synthesized alloy are reported.

2. Experimental procedure

Irregular titanium powders and nickel powders were used in this study. The powders were of a commercially

‡ Author to whom all correspondence should be addressed.
* Also Beijing Laboratory of Electron Microscopy, Chinese Academy of Sciences, P.O. Box 2724, Beijing 100080, People's Republic of China.

pure grade, as indicated elsewhere [8]. After thoroughly mixing, the mixture of the two powders was pre-pressed between a stainless steel core and a stainless steel tube which were coaxially located to obtain an appropriate pre-porosity. The pre-pressing was performed on a bed of sand. The detonation velocity was nearly 6500 $m\,s^{-1}$. After explosion, the metallic bar and steel tube were mechanically removed. Quantitative elemental composition analysis was carried out using an energy dispersive X-ray spectroscope (EDXS). The state of the compacts was identified by X-ray diffractometry and transmission electron microscopy (TEM). The as-synthesized specimens for TEM observation were prepared by ion thinning and observations were carried out on a Philips EM 430 with a double-tilting goniometer. The phase-transformation behaviour was studied by utilizing differential scanning calorimeter (DSC) analyser at a heating and cooling rate of 10 $^{\circ}C\,min^{-1}$ on a Dupont 2000 DSC thermal analyser. The transition temperatures were determined as the extrapolated onset temperatures.

3. Results

3.1. X-ray diffraction analysis

Fig. 1(a) shows X-ray diffraction pattern of the prepressed specimen before explosion which consists of pure nickel and pure titanium patterns. After explosive compression, diffraction peaks characteristic of pure titanium and nickel elements completely disappeared, and were substituted by peaks characteristic of TiNi intermetallic compound, as shown in Fig. 1b, where the (1 1 0), (2 0 0), (2 1 1) peaks of B2 type parent phase with a lattice parameter $a = 0.301$ nm are evident. Moreover, diffraction peaks of R phase, B19′ type martensite and Ti_2Ni phase can also be indexed. Fig. 1c is the pattern of the synthesized sample after ageing at room temperature (RT) for 2 weeks. Note that the peaks in Fig. 1b are broader than those in Fig. 1c. This fact indicates a strong residual internal strain existing in the as-synthesized specimen which can be partly removed by RT ageing.

3.2. TEM observation

Fig. 2a is bright-field (BF) image showing the morphology of the Ti_2Ni particles (arrowed) coexisting with the matrix. Fig. 2b is a selected-area electron diffraction pattern (EDP) taken from the matrix which is a typical [1 0 0] B2 EDP with $a \simeq 0.301$ nm, in agreement with TiNi B2 type parent phase. Fig. 2c–e show EDPs taken from the arrowed particle B along, respectively, the [1 0 0], [1 $\bar{1}$ 0] and [$\bar{1}$ 1 1] zone axes of a face-centred cubic (f c c) phase with a lattice parameter of $a = 1.13$ nm. The reflection spots in the (1 0 0)* reciprocal plane (Fig. 2c), revealing an additional reflection condition $h + k + l = 4n$, indicate that the space group should be $Fd\bar{3}\,m$, which is in good agreement with that of the Ti_2Ni phase [9]. By comparing Fig. 2c and d one can interpret the appearance of the forbidden reflections (0 0 $\bar{2}$), (2 2 $\bar{2}$), … , in

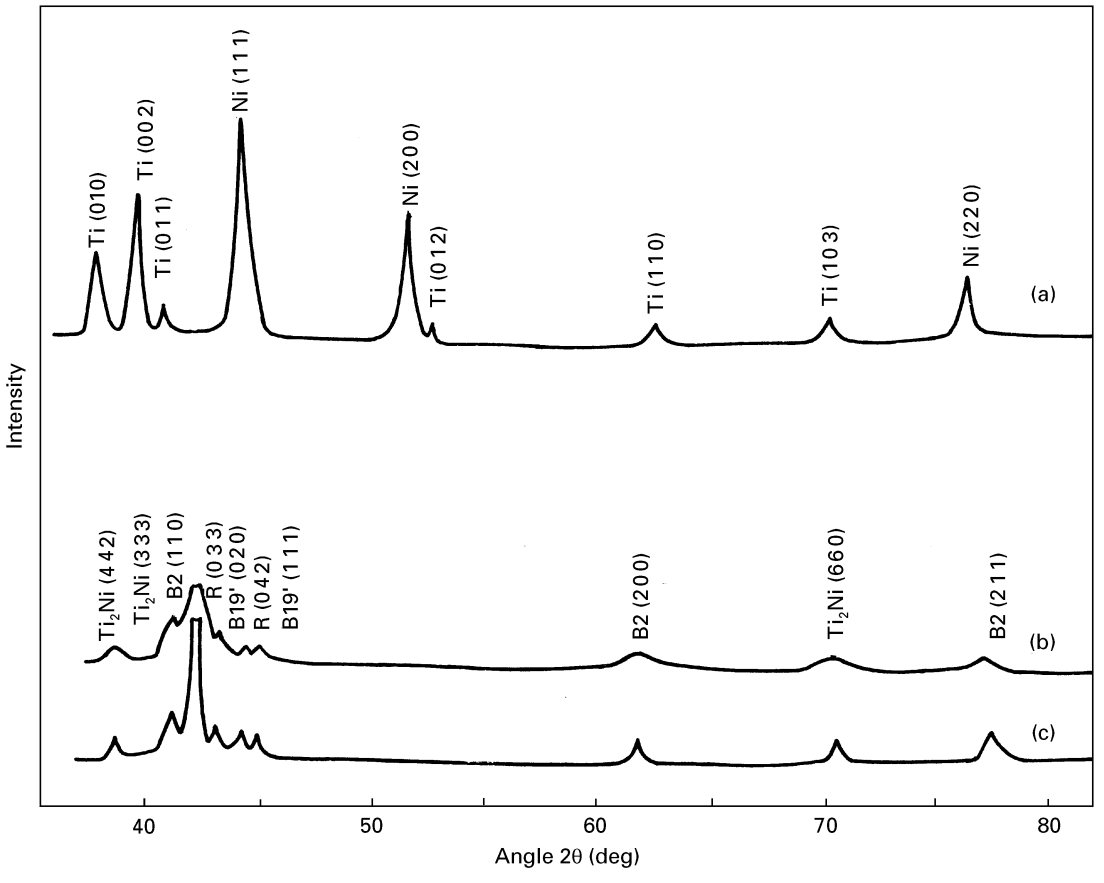

Figure 1 X-ray diffraction patterns: (a) pre-pressed sample before explosion; (b) as-synthesized sample; (c) synthesized sample after RT ageing.

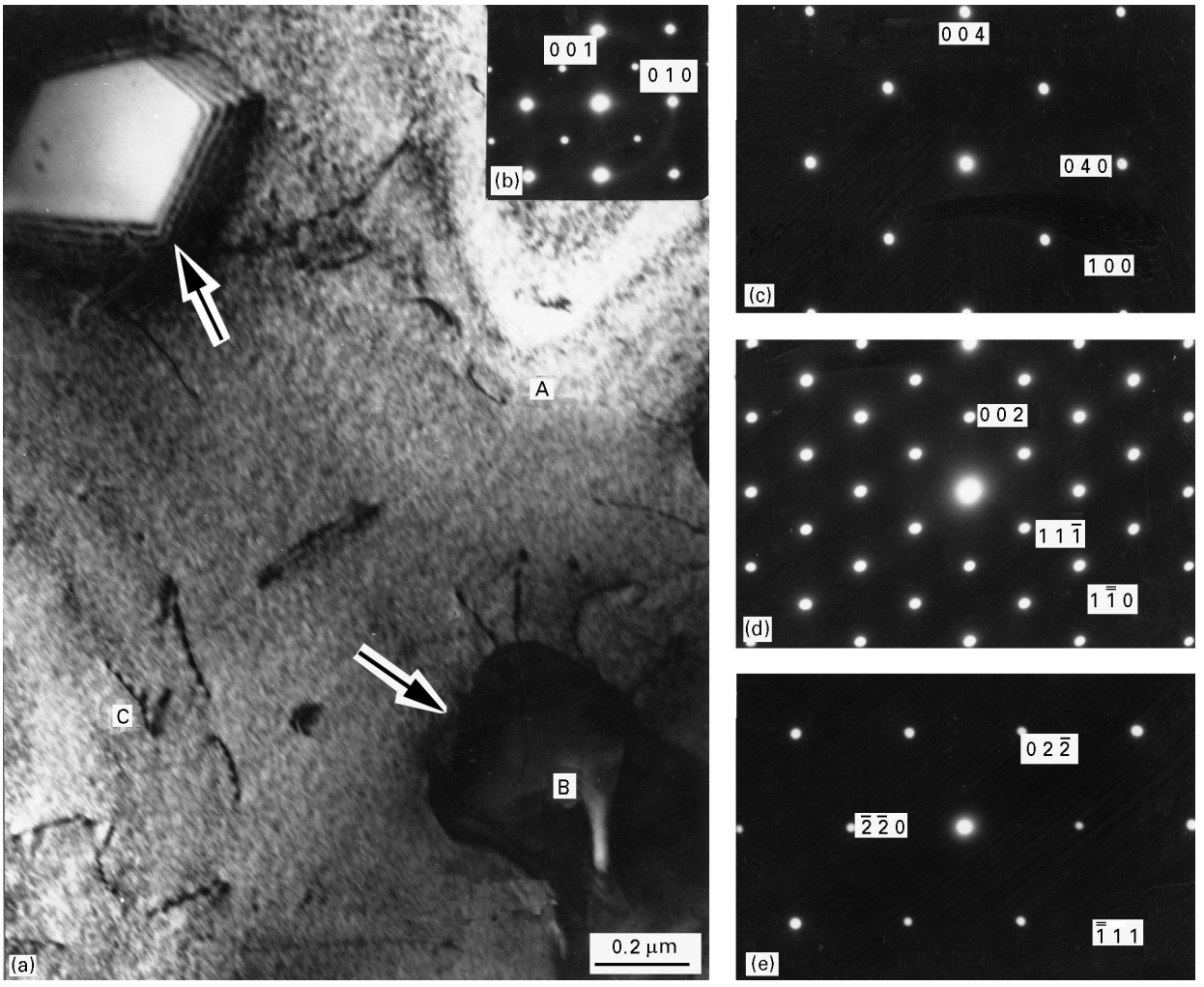

Figure 2 General morphology of the as-synthesized TiNi alloy. (a) BF image showing Ti_2Ni particles (arrowed), dislocations and stacking fault (region C) in the matrix. (b) [1 0 0] (B2) EDP taken from region A. (c) [1 0 0] (Ti_2Ni) EDP. (d) [1 $\bar{1}$ 0] (Ti_2Ni) EDP. (e) [$\bar{1}$ 1 1] (Ti_2Ni) EDP. (c–e) are taken from particle B.

Fig. 2d by multiple scattering. EDXS measurement of these particles revealed the atomic ratio of Ni : Ti = 1 : 2 without oxygen, which confirmed the identification of Ti_2Ni.

In some regions there are satellite reflections of $1/7\langle 3\,2\,1\rangle^*$ and $1/7\langle 4\,2\,1\rangle^*$ types accompanying strong B2-type reflections as shown in Fig. 3a–c which are along the [$\bar{2}$ 1 1] [$\bar{1}$ 1 1] and [$\bar{3}$ 4 4] zone axes of the B2-type matrix, respectively. The appearance of $1/7[0\,1\,\bar{1}]^*$ reflection in Fig. 3c may be interpreted by multiple scattering: $1/7[4\,2\,1]^* + 1/7[\bar{4}\,\bar{1}\,\bar{2}]^* = 1/7[0\,1\,\bar{1}]^*$. These satellite reflections are characteristic of the rhombohedral Ti_3Ni_4 (or $Ti_{11}Ni_{14}$) precipitate [10] with the lattice parameters of $a = 0.670$ nm and $\alpha = 113.8^\circ$, which possesses the following lattice correspondence with the B2 type parent phase

$$[a\ b\ c]_{Ti_3Ni_4} = [a\ b\ c]_{B_2}\boldsymbol{P} \tag{1}$$

with

$$\boldsymbol{P} = \begin{bmatrix} 2 & -1 & 0 \\ 0 & 2 & -1 \\ -1 & 0 & 2 \end{bmatrix} \tag{2}$$

from Equations 1 and 2 it is easy to deduce the reciprocal lattice correspondence

$$\begin{bmatrix} a^* \\ b^* \\ c^* \end{bmatrix}_{Ti_3Ni_4} = \boldsymbol{Q}\begin{bmatrix} a^* \\ b^* \\ c^* \end{bmatrix}_{B2} \tag{3}$$

with

$$\boldsymbol{Q} = \boldsymbol{P}^{-1} = \frac{1}{7}\begin{bmatrix} 4 & 2 & 1 \\ 1 & 4 & 2 \\ 2 & 1 & 4 \end{bmatrix} \tag{4}$$

and the following orientation relationships

$$\begin{aligned} [1\ 1\ 1]_{B2} &= [1\ 1\ 1]_{Ti_3Ni_4} \\ \frac{1}{7}(2\ 1\ \bar{3})_{B2} &= (1\ 0\ \bar{1})_{Ti_3Ni_4} \\ \frac{1}{7}(4\ 2\ 1)_{B2} &= (1\ 0\ 0)_{Ti_3Ni_4} \end{aligned} \tag{5}$$

Fig. 3d is a dark-field (DF) image showing the irregular morphology of these Ti_3Ni_4 precipitates.

In addition to the B2 matrix, we have occasionally observed some lenticular particles (Fig. 4a) where

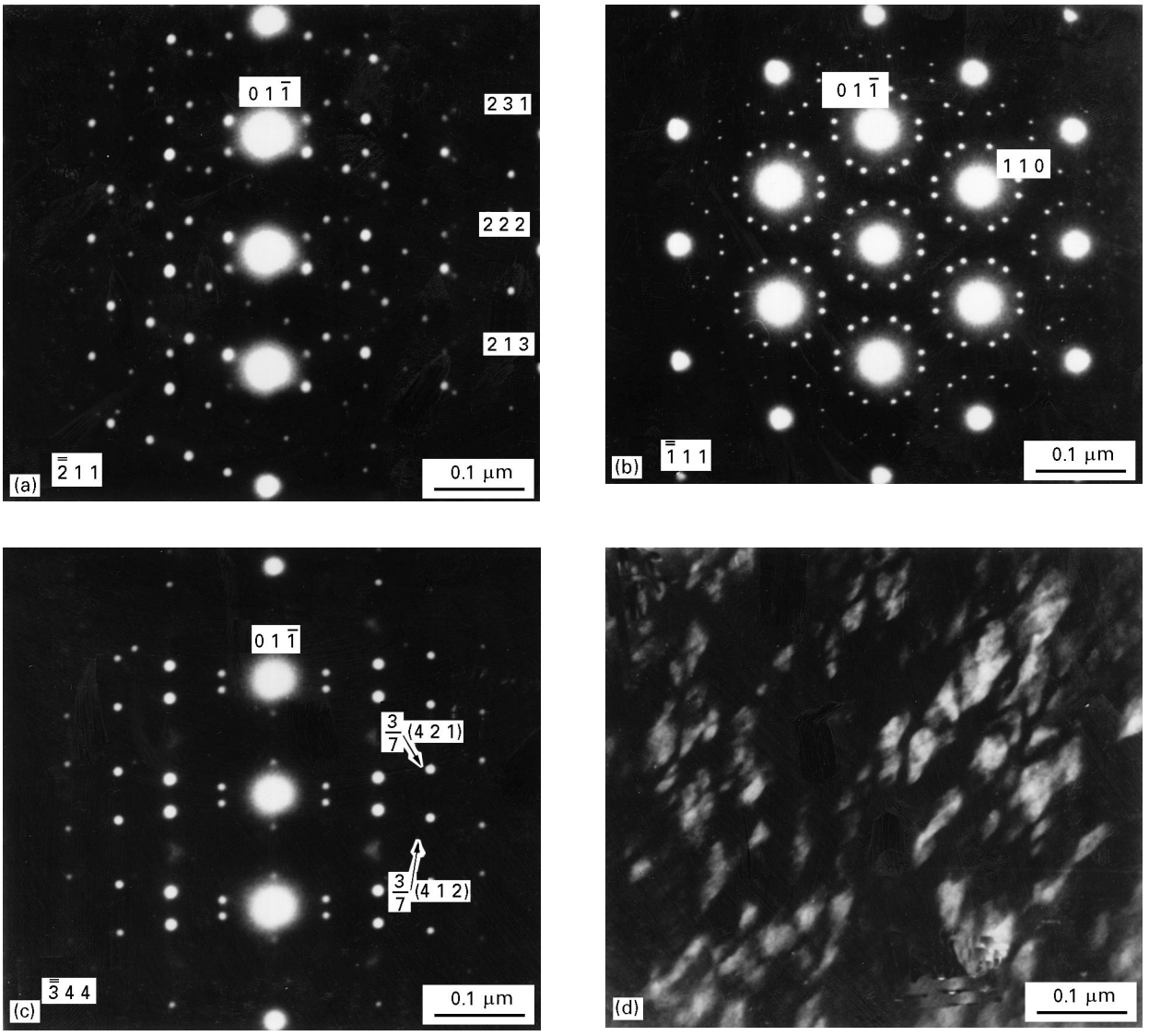

Figure 3 EDPs and DF image showing Ti_3Ni_4 precipitates distributed in the B2 parent phase. (a) $[\bar{2}\,1\,1]$ (B2) EDP. (b) $[\bar{1}\,1\,1]$ (B2) EDP. (c) $[\bar{3}\,4\,4]$ (B2) EDP. (d) DF image.

Moiré patterns (arrowed) at the border region can be seen. Fig. 4b–d show EDPs along, respectively, the [0 0 1], [1 1 1], and [0 1 1] zone axes of the B2 matrix with a lattice parameter $a = 0.301$ nm. Besides strong reflections from the B2 matrix, weak reflections from another B2-type phase with a lattice parameter $a \simeq 0.887$ nm are clearly seen. EDXS was employed to study the composition of this kind of particle. The results indicate that the particles contain no oxygen element, and the atomic ratio of titanium to nickel is nearly 2:3, so this kind of particle can be expressed as the Ti_2Ni_3 phase. Obviously the Moiré patterns result from the difference of the lattice-plane distances between TiNi matrix and Ti_2Ni_3 particles. The results of EDXS also indicate that the elemental distribution in the matrix is inhomogeneous, some area is nickel-rich and some area is titanium-rich. The influence of the inhomogeneous elemental distribution on phase-transformation behaviour of this synthesized alloy will be discussed later in this paper.

At room temperature, although the majority of the as-synthesized TiNi alloy is B2 parent phase, we have also found some R phase (region B in Fig. 5a) and B19′ type martensite (region A). Fig. 5b is an EDP from region B where we clearly see 1/3 $\{1\,1\,0\}$ B2 satellite reflections characteristic of two variants of the R phase forming (1 0 0) B2 twin. Fig. 5c is an EDP from region A which can be indexed as [1 1 0] B19′ zone-axis EDPs with a (0 0 1) B19′ twin structure. In addition, there are strong diffuse streaks along the [0 0 1]*B19′ plane, indicating that there are either stacking faults or (0 0 1) B19′ microtwins along this plane, as shown in region A in Fig. 5a.

In addition to the strong internal strain field as revealed by the broad X-ray diffraction peaks shown in Fig. 1b, there are many isolated (see Fig. 2a) and tangled (not shown) dislocations and stacking faults (see region C in Fig. 2a) in the matrix. Preliminary contrast experiments identified Burgers vectors of many dislocations to be parallel to the $\langle 1\,1\,1 \rangle$ B2 direction.

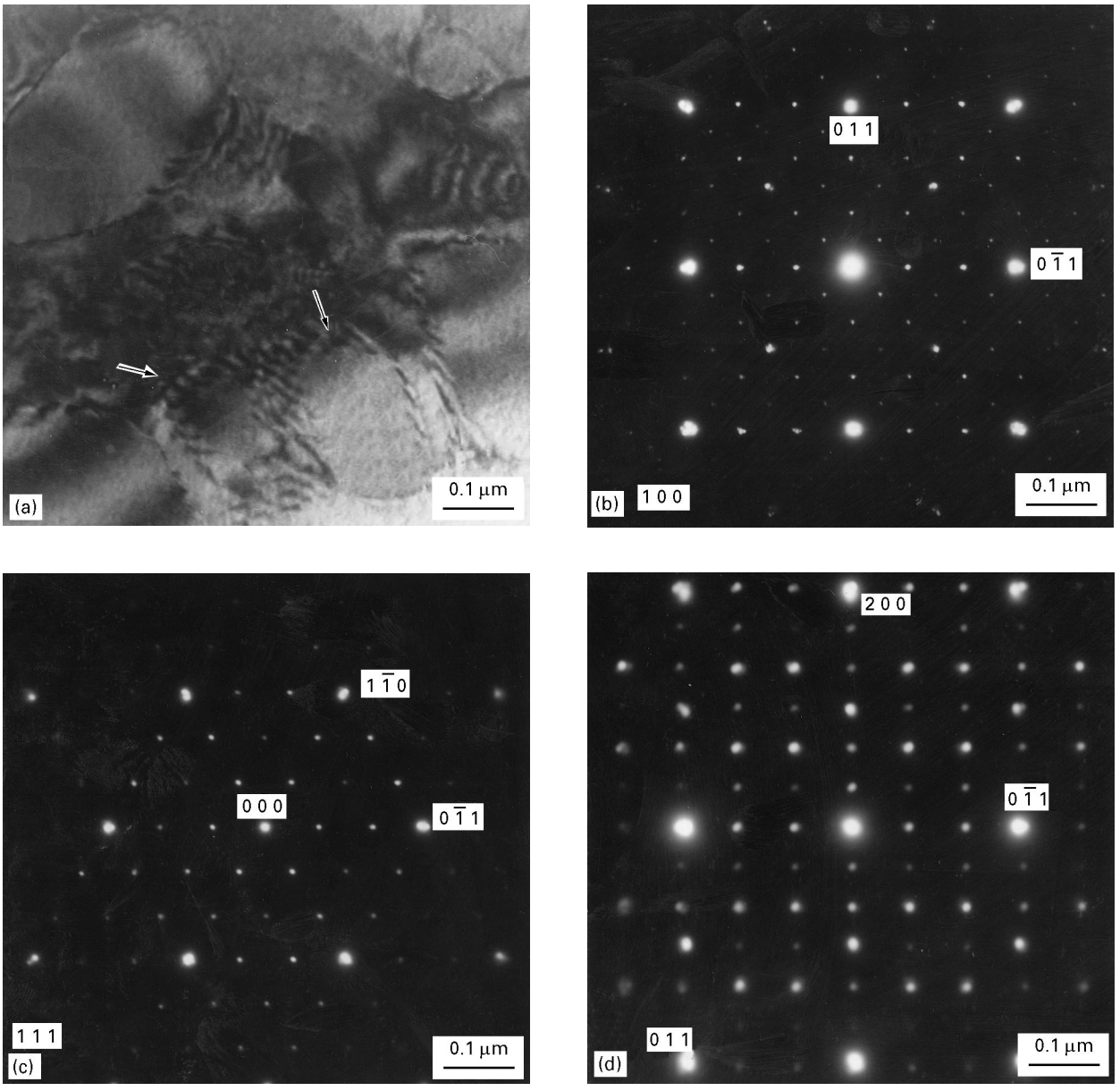

Figure 4 BF image and EDPs of cubic Ti_2Ni_3 particles with $a \simeq 0.887$ nm distributed in B2-type parent phase. (a) BF image. (b) [1 0 0] (B2) EDP. (c) [1 1 1] (B2) EDP. (d) [0 1 1] (B2) EDP.

3.3. DSC measurement

When increasing the temperature of the as-synthesized TiNi alloy in the DSC analyser from -50 to 100 °C, no phase transformation was observed. During the cooling cycle we observed B2 → R → B19′ transitions with $M_s = 25$ °C and $M_f = -16$ °C. After the alloy was heat treated at 800 °C for 1 h and then 400 °C for 10 min, DSC experiments showed both B19′(R) → B2 and B2 → R → B19′ transitions with the following critical temperatures: $T_R = 55$ °C, $M_s = 17$ °C, $M_f = 2$ °C, $A_s = 27$ °C, $A_f = 66$ °C.

4. Discussion

The present work shows clearly that TiNi SMA can be synthesized by means of explosive shock-wave compression from mixed powders of pure titanium and pure nickel elements. Compared with our previous work [8, 11] we find that it needs a very high detonation velocity to initiate a complete chemical reaction by an explosive shock wave.

According to the TiNi binary alloy phase diagram, the Ti_2Ni and $TiNi_3$ phase cannot exist simultaneously in the TiNi matrix. Ti_2Ni exists at the titanium-rich side, while $TiNi_3$ phase exists in the nickel-rich side. The Ti_3Ni_4 non-equilibrium phase also exists in the nickel-rich side, and it could not be formed unless the nickel content is higher than 50.6% [12]. However, in the TiNi alloy synthesized by explosion, a large amount of Ti_2Ni and Ti_3Ni_4 phases and occasionally some Ti_2Ni_3 particles were found in the TiNi matrix. EDP of Ti_2Ni_3 particles (Fig. 4) still show cubic symmetry, in contrast with the equilibrated Ti_2Ni_3 phase, which was reported to be tetragonal, or orthogonal, or monoclinic crystals [13]. These phenomena are related to the inhomogeneous composition of the as-synthesized alloy and the high cooling velocity after explosion. The conventional

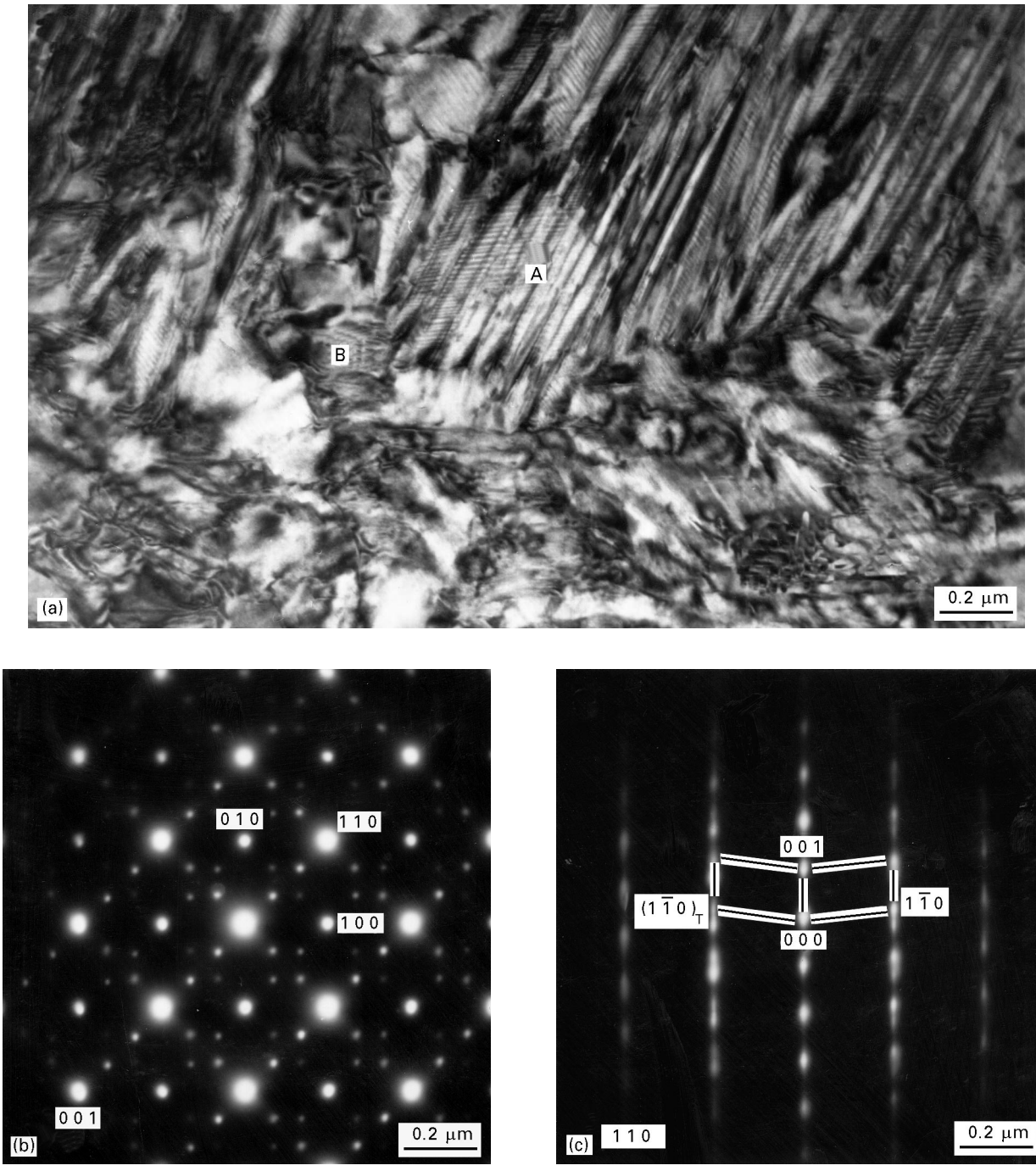

Figure 5 BF image and EDPs showing parent phase and B19′ martensite. (a) BF image. (b) [0 0 1] (B2) EDP taken from region B showing $1/3\langle 1\,1\,1\rangle^*$ type satellite reflections characteristic of R phase. (c) [1 1 0] (B19′) EDP taken from region A showing (0 0 1) B19′ twin structure.

diffusion in the melt and solid could not occur, hence both the nickel-rich and titanium-rich areas can exist.

It is well known that the M_s temperature of Ti–Ni SMA decreases with the increasing nickel content. Therefore, the broad transformation temperature range ($M_s - M_f = 41\,^{\circ}C$) in the as-synthesized TiNi SMA as measured by DSC, can be interpreted by the inhomogeneous composition of the as-synthesized specimen. After heat treatment at 800 °C for 1 h, the composition of the matrix will be homogenized and the transition temperature range becomes narrowed. Therefore, it can be concluded from the present study that a homogenization treatment should be performed to obtain a stable phase transformation behaviour for the explosively synthesized TiNi SMA.

Acknowledgements

This project has been supported by the National Natural Science Foundation of China.

References

1. M. IGHARO and J. V. WOOD, *Powder Metall.* **28** (1986) 131.
2. H. C. YI and J. J. MOOR, *Scripta Metall.* **22** (1988) 1889.
3. W.H. GOURDIN, *Progr. Mater. Sci.* **30** (1986) 39.
4. N. N. THADHANI, *Adv. Mater. Manuf. Proc.* **3** (1988) 493.
5. G. E. DUVALL and R. A. GRAHAM, *Rev. Mod. Phys.* **49** (1977) 523.
6. Y. M. RYABININ, *Sov. Phys. Tech. Phys.* **1** (1956) 2575.
7. A. N. DREMIN and O. N. BRUESOV, *Russ. Chem. Rev.* **37** (1968) 392.

8. T. C. LI, Y. B. QIU, J. T. LIU and D. Z. YANG, *J. Mater. Sci. Lett*. **11** (1992) 847.
9. M. H. MUELLER and H. W. KNOTT, *Trans. Met. Soc. AIME* **227** (1963) 674.
10. M. NISHIDA, C. M. WAYMAN, R. KAINUMA and T. HONMA *Scripta Metall.* **20** (1986) 899.
11. M. ZHU, T. C. LI, J. T. LIU and D. Z. YANG, *Acta. Metall. Mater*. **39** (1991) 1481.
12. S. MIYAZAKI, Y. OHMI, K. OTSUKA and Y. SUZUKI, *J. Phys. Suppl.* **43** Dec (1982) C4-255.
13. M. NISHIDA and C. M. WAYMAN, *Metall Trans.* **18A** (1987) 785.

Received 12 April 1995
and accepted 28 January 1996